Neuron, Vol. 24, 261–273, September, 1999, Copyright ©1999 by Cell Press

Activation of a TRPC3-Dependent Cation Current through the Neurotrophin BDNF

Hong-Sheng Li, Xian-Zhong Shawn Xu, and Craig Montell*
Departments of Biological Chemistry and Neuroscience
The Johns Hopkins University School of Medicine
Baltimore, Maryland 21205

Summary

Nonvoltage-gated cation currents, which are activated following stimulation of phospholipase C (PLC), appear to be major modes for Ca^{2+} and Na^{+} entry in mammalian cells. The TRPC channels may mediate some of these conductances since their expression in vitro leads to PLC-dependent cation influx. We found that the TRPC3 protein was highly enriched in neurons of the central nervous system (CNS). The temporal and spatial distribution of TRPC3 paralleled that of the neurotrophin receptor TrkB. Activation of TrkB by brain-derived nerve growth factor (BDNF) led to production of a PLC-dependent, nonselective cation conductance in pontine neurons. Evidence is provided that TRPC3 contributes to this current in vivo. Thus, activation of TrkB and PLC leads to a TRPC3-dependent cation influx in CNS neurons.

Introduction

Influx of Ca^{2+} and Na^{+} is essential in the nervous system for propagation of action potentials, synaptic transmission, synaptic plasticity, and development (reviewed by Berridge, 1998). In nonexcitable cells, cation influx appears to function in processes ranging from the immune response to cell growth and development (reviewed by Parekh and Penner, 1997). A wide variety of voltage-, ligand-, and second messenger–gated channels have been identified that mediate Ca^{2+} and Na^{+} influx in excitable cells (reviewed by Jan and Jan, 1992). However, the ion channels and gating mechanisms regulating the Ca^{2+}-selective and -nonselective cation conductances in nonexcitable cells have been more elusive.

A growing body of evidence indicates that many of the cation conductances in nonexcitable cells are coupled to the activation of phospholipase C (PLC). However, the mechanisms by which activation of PLC leads to cation influx have not been resolved. A prevailing model is that production of inositol 1,4,5-trisphosphate, through hydrolysis of phosphatidylinositol 4,5-bisphosphate, leads to transient release of Ca^{2+} from internal Ca^{2+} stores, which in turn induces a sustained Ca^{2+}-selective or -nonselective cation influx (Putney and Bird, 1994; Berridge, 1995; Parekh and Penner, 1997). Nevertheless, there is evidence that some PLC-dependent cation influx pathways operate independently of the Ca^{2+} stores (reviewed by Parekh and Penner, 1997).

Identification of the channels mediating the store-operated and other PLC-dependent conductances has generated considerable interest, and vertebrate homologs of the *Drosophila* TRP channel have emerged as candidates. TRP is expressed predominantly in photoreceptor cells (Montell et al., 1985; Montell and Rubin, 1989) and is a subunit of a light-dependent channel that is permeable primarily to Ca^{2+} and to a lesser extent, Na^{+} (Hardie and Minke, 1992). Activation of TRP is strictly dependent on PLC since mutations that remove the PLC expressed in photoreceptor cells obliterate the light-induced cation influx (reviewed by Montell, 1999). Moreover, TRP can be activated in vitro through a store-operated mechanism (Vaca et al., 1994; Peterson et al., 1995; Xu et al., 1997). Six vertebrate homologs of TRP (TRPC proteins) have been identified (Wes et al., 1995; Zhu et al., 1995, 1996), each of which has been expressed functionally in vitro (Philipp et al., 1996; Zhu et al., 1996; Zitt et al., 1996; Boulay et al., 1997; Okada et al., 1998; Philipp et al., 1998; Vannier et al., 1999). Some TRPC channels appear to be coupled in vitro to store depletion (Philipp et al., 1996); however, others may not be. Recently, evidence has been provided that TRPC3 is activated through a store-operated mechanism (Hofmann et al., 1999), although another in vitro study has implicated diacylglycerol (DAG) as the second messenger that regulates TRPC3 (Kiselyov et al., 1998). The TRPC conductances also display variations in selectivity. While TRPC4 and TRPC5 are relatively Ca^{2+} selective (Philipp et al., 1996, 1998; Okada et al., 1998), the remaining TRPC conductances are nonselective (e.g., Zitt et al., 1997; Zhu et al., 1998). Nevertheless, a feature common among all of the TRPC channels is that each is activated in vitro through signaling pathways that utilize PLC.

Considering that most store-operated and PLC-dependent cation conductances have been described in nonexcitable cells (reviewed by Putney, 1993), an unexpected finding is that at least five of the six *TRPC* RNAs are expressed in the brain (Garcia and Schilling, 1997). Moreover, three *TRPC* RNAs, *TRP3*, *TRPC4*, and *TRPC5*, are highly enriched in the brain (Funayama et al., 1996; Zhu et al., 1996; Mori et al., 1998; Philipp et al., 1998). These observations raise questions as to the function of TRPC proteins in the brain and the nature of the signaling pathways that are coupled to the activation of these channels in the central nervous system (CNS). Since all known *Drosophila* and vertebrate TRP conductances are dependent on PLC, candidate signaling pathways include those that are linked to the activation of PLC.

In the current report, we show that the TRPC3 protein is expressed predominantly in CNS neurons during a relatively narrow developmental window before and after birth. The spatial distribution of TRPC3 was similar to the pattern of the neurotrophin receptor TrkB (Klein et al., 1989; Fryer et al., 1996; Yan et al., 1997; Fariñas et al., 1998). Neurotrophin receptors induce a variety of

*To whom correspondence should be addressed (e-mail: cmontell@jhmi.edu).

effects in the nervous system, including neuronal differentiation, cell proliferation, cell survival, and modulation of neurotransmitter release at developing synapses (reviewed by Lo, 1995; Thoenen, 1995; Henderson, 1996; Reichardt and Fariñas, 1997; Shieh and Ghosh, 1997). Since TrkB is a receptor tyrosine kinase (RTK) that engages PLCγ1 (reviewed by Segal and Greenberg, 1996), it seemed plausible that activation of TrkB by the neurotrophin brain-derived neurotrophic factor (BDNF) might lead to a TRPC3-mediated cation conductance that is dependent on PLC. We found that application of BDNF to primary CNS neurons resulted in the appearance of a nonspecific cation conductance that required activation of PLC. Moreover, we provide evidence that TRPC3 is a subunit that contributes to this conductance. Thus, it appears that one signaling pathway that leads to the activation of TRPC3 in CNS neurons involves neurotrophin receptors and PLCγ1.

Results

Expression of TRPC3 in the CNS Around the Time of Birth

To determine the temporal expression and spatial distribution of the TRPC3 protein, we raised chicken polyclonal antibodies to the N-terminal 213 residues of TRPC3 (Zhu et al., 1996). The αTRPC3^{N213} antibodies appeared to be specific to the 848 amino acid TRPC3 protein since they recognized the same ~92 kDa TRPC3–Myc protein expressed in 293T cells as the anti-Myc antibodies (Figure 1A). Furthermore, αTRPC3^{N213} did not cross-react with a highly related vertebrate TRPC homolog, TRPC1 (Figure 1A).

TRPC3 RNA has previously been shown to be enriched in the adult human or mouse brain (Zhu et al., 1996; Mori et al., 1998). However, we found that the TRPC3 protein was predominantly expressed in the rat brain during a relatively narrow developmental period before and after birth. TRPC3 protein was detected 3 days prior to birth on embryonic day 18 (E18; Figure 1B) and continued to be expressed until postembryonic day 20 (P20). A similar expression pattern occurred in mice (data not shown). In addition, TRPC3 was expressed in human fetal but not in adult cerebral cortices (Figure 1C). Thus, the TRPC3 protein was not expressed in the adult brain despite the presence of *TRPC3* RNA in adults.

The *TRPC3* RNA is enriched in the brain and detected at lower levels in many peripheral tissues (Zhu et al., 1996; Garcia and Schilling, 1997; Mori et al., 1998). However, the TRPC3 protein was not detected in the heart, lung, liver, kidney, spleen, stomach, intestine, muscle, or skin (Figure 1D). In addition, the TRPC3 protein did not appear to be expressed in those portions of the peripheral nervous system, such as the dorsal root ganglia (DRG), that were examined in this analysis (Figure 1E). However, a positive signal was observed in a wide variety of tissues in the CNS (Figure 1E). Therefore, it appeared that TRPC3 was predominantly expressed in the CNS.

TRPC3 Was Spatially Localized to CNS Neurons

To spatially localize TRPC3, we stained sections of neonatal rat brains with αTRPC3^{N213} antibodies. No signal was detected with chicken immunoglobulin Y (IgY) that did not contain TRPC3 antibodies (data not shown). However, the TRPC3 antibodies specifically stained subsets of many brain tissues, including the cerebral cortex, hippocampus, thalamus, hypothalamus, and amygdala (Figures 2A and 2C); the cerebellum, midbrain, and pons (Figure 2E); and the olfactory bulb (Figure 2G). Within these tissues, it appeared that TRPC3 was expressed predominantly in neurons. These included pyramidal neurons in the cerebral cortex (Figure 3A) and hippocampus (Figure 3C), neurons in the amygdala (Figure 3E), and Purkinje cells in the cerebellum (Figure 3G). The αTRPC3^{N213} staining occurred in cell bodies and dendrite-like neurites. No TRPC3 was observed in glial cells.

TRPC3 Colocalized with the BDNF Receptor TrkB in Fetal and Neonatal Rat Brains

The mechanism by which TRPC3 is activated in vivo is not known. However, TRPC3 can be activated in vitro by stimulation of G protein–coupled receptors that associate with PLCβ (Zhu et al., 1996; Zitt et al., 1997). To identify a potential mode through which TRPC3 might be activated in vivo, we considered neuronal membrane receptors that display the same spatial and temporal expression patterns as TRPC3, or overlapping patterns, and that are linked to PLC. One such candidate is the RTK TrkB, which is activated by the neurotrophin BDNF and which associates with PLCγ1 (reviewed by Barbacid, 1995; Segal and Greenberg, 1996). Expression of TrkB appeared to peak around the time of birth (E18–P10; Figures 1F and 1G). However, TrkB can be detected throughout adulthood if the protein is first concentrated by performing immunoprecipitations with pan-Trk antibodies prior to the Western blot analysis (Fryer et al., 1996). Peak levels of TRPC3 also occurred between E18 and P10 (Figure 1B). The concentration of TRPC3 was reduced in the P20 sample and could not be detected at later stages.

To determine whether TRPC3 and TrkB were expressed in the same neurons, we stained parallel sections from the neonatal rat brain with antibodies to each protein. The spatial distribution of TrkB was indistinguishable from that obtained with the TRPC3 antibodies in both P4 and P10 brain sections (Figure 2). Consistent with previous analyses (Yan et al., 1997), the TrkB antibodies stained the cell bodies and dendrite-like neurites of neurons in the cerebral cortex (Figure 3B), hippocampus (Figure 3D), and amygdala (Figure 3F). To determine whether TRPC3 and TrkB were expressed in the same neurons, we performed double-labeling experiments on both brain sections (Figures 3G and 3H) and isolated pontine neurons (Figures 3I and 3J). We found that TRPC3 and TrkB were expressed in the same Purkinje cells in the cerebellum and pontine neurons and had the same subcellular localization (Figures 3G–3J). Most pontine neurons (81.2%) expressed both TRPC3 and TrkB, while only a few expressed just TRPC3 (3.9%) or TrkB (4.9%), or neither protein (10.0%). Thus, TRPC3 and TrkB appeared to be expressed in the same cells.

BDNF-Activated a Ca^{2+}-Dependent Nonselective Cation Conductance in Pontine Neurons

Based on in vitro studies, the TRPC channels are nonvoltage gated, PLC dependent cation channels. To determine whether application of BDNF induced a current

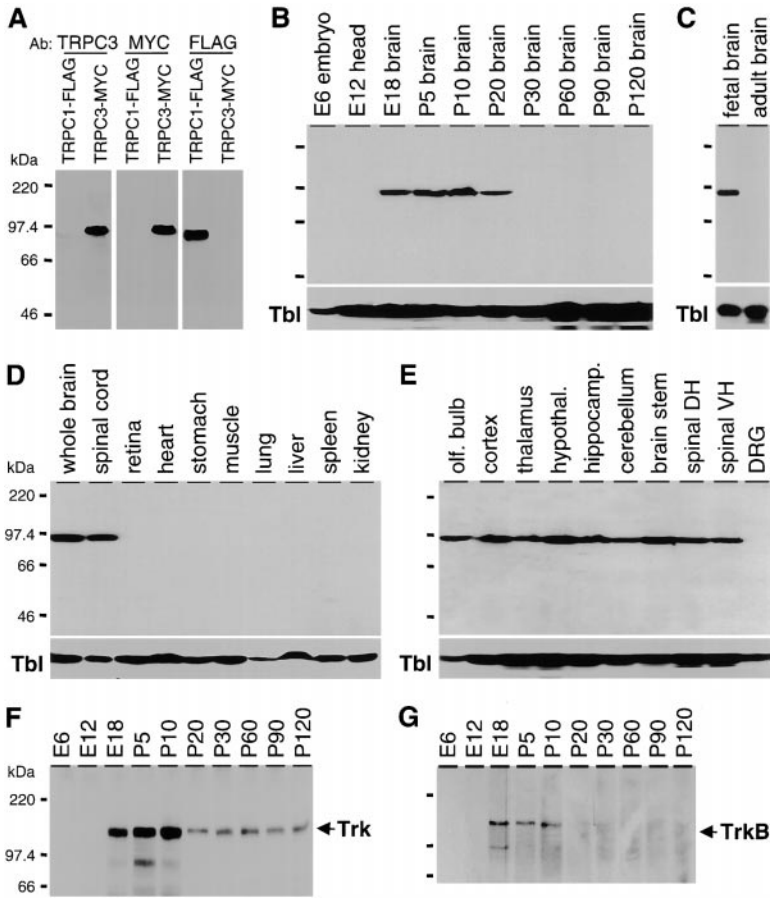

Figure 1. Western Blots Indicating the Expression Pattern of TRPC3

Extracts were prepared from the indicated tissues or from 293T cells and fractionated by SDS–PAGE, and Western blots were probed with either anti-Myc (A), anti-Flag (A), anti-TRPC3 (A–E), pan-Trk (F), or anti-TrkB antibodies (G). The positions of the 220, 97.4, 66, and 46 kDa protein size markers are indicated.

(A) Anti-TRPC3 antibodies recognize TRPC3 but not TRPC1 (fused to Myc and FLAG tags, respectively) expressed in 293T cells.

(B) Expression of TRPC3 in the rat brain during development and in the adult. Extracts were prepared from embryonic (E) and postnatal (P) rats at the times indicated. E6 and E12 extracts were prepared from whole embryos and heads, respectively. Brain tissue was used for all other samples. After probing with anti-TRPC3 antibodies, this and subsequent blots were reprobed with antibodies that recognize α- and β-tubulin (Tbl).

(C) TRPC3 was expressed in the brain of a 19-week-old human fetus but not in the brain of a 44-year-old adult.

(D) TRPC3 was detected in the brain and spinal cord but not in peripheral tissues from a P5 rat.

(E) TRPC3 was expressed in many regions of a P10 rat brain.

(F) Developmental expression of TrK. The same samples used in (B) were probed with pan-Trk antibodies, which recognize TrkA, TrkB, and TrkC.

(G) TrkB is expressed around birth. Samples identical to those used in (B) were probed with anti-TrkB antibodies.

reminiscent of TRPC channels, we applied BDNF to isolated rat pontine neurons and performed whole-cell recordings. Application of BDNF for 30 s produced a delayed (1.2 ± 0.6 min, $n = 16$ of 18) inward current (I_{BDNF}) with an amplitude of 6.8 ± 1.4 pA/pF at -70 mV (Figures 4A and 4G). The cells died after 25 ± 7 min ($n = 8$ of 8) before there was significant diminution of the current (Figure 4B). The cell death may have been due to entry of toxic levels of cations. Nevertheless, using a different paradigm, it appeared that I_{BDNF} did not proceed indefinitely. After adding BDNF and establishing I_{BDNF}, the current was greatly reduced as a consequence of switching the voltage clamp from -70 to -30 mV (Figure 4C). Upon returning the clamp to -70 mV after 27 min, the current was partially restored but was greatly diminished (reduced to $16.5\% \pm 5.8\%$ of the original current, $n = 4$ of 5) and subsequently terminated in 4.3 ± 1.6 min. The duration of I_{BDNF} under these conditions was 33 ± 4 min. I_{BDNF} was consistently blocked ($n = 6$ of 6) by addition of the Trk inhibitor K252a (Figures 4E and 4G). Upon withdrawal of the inhibitor, the inward current could then be induced by BDNF. The effect of BDNF did not appear to be nonspecific since addition of the agonists for the δ opioid receptor (DADLE; $n = 9$) or for two other RTKs known to be expressed in pontine neurons (brain fibroblast growth factor receptor [bFGFR], $n = 6$; insulin growth factor receptor [IGFR], $n = 5$) had no apparent effect on any of the cells tested (Figures 4D and 4G).

Although bFGFR and IGFR did not stimulate cation influx, another neurotrophin, NT-3, which binds primarily to TrkC and to a lesser extent, TrkB (Fariñas et al., 1998), produced a current similar to but smaller than that of BDNF (data not shown). As expected, since TrkA is not expressed in the pons (Martin-Zanca et al., 1990), application of the agonist for TrkA, nerve growth factor (NGF; reviewed by Reichardt and Fariñas, 1997) did not induce any inward current (Figures 4D and 4G; $n = 7$ of 7 cells). Nevertheless, stimulation of TrkA did not appear to lead to a similar nonselective cation influx since there was no induction of cation influx upon addition of the TrkA ligand NGF to a cell line, PC-12 cells, that expressed TrkA (H.-S. L. et al., unpublished data).

I_{BDNF} was a cation current but was not Ca^{2+} selective since elimination of Na^+ and Mg^{2+} from the extracellular solution decreased the current nearly to the baseline (Figures 4F and 4G; 0.9 ± 0.2 pA/pF, $n = 7$ of 8). The remaining current appeared to be carried by Ca^{2+} since this was the only cation present in the bath solution. Therefore, this current was carried mainly by Na^+, while Ca^{2+} contributed to a lesser extent. After blocking the voltage-gated K^+ and Na^+ channels with 140 mM CsCl and 2 μM tetrodotoxin, respectively, a set of step voltages was applied to determine the I–V relationship. The I–V curves showed that the reversal potential was around 4 mV in an extracellular solution containing Na^+ as the sole permeant cation (Figure 4H; $n = 7$). Because Mg^{2+} did not appear to carry this current and was in very

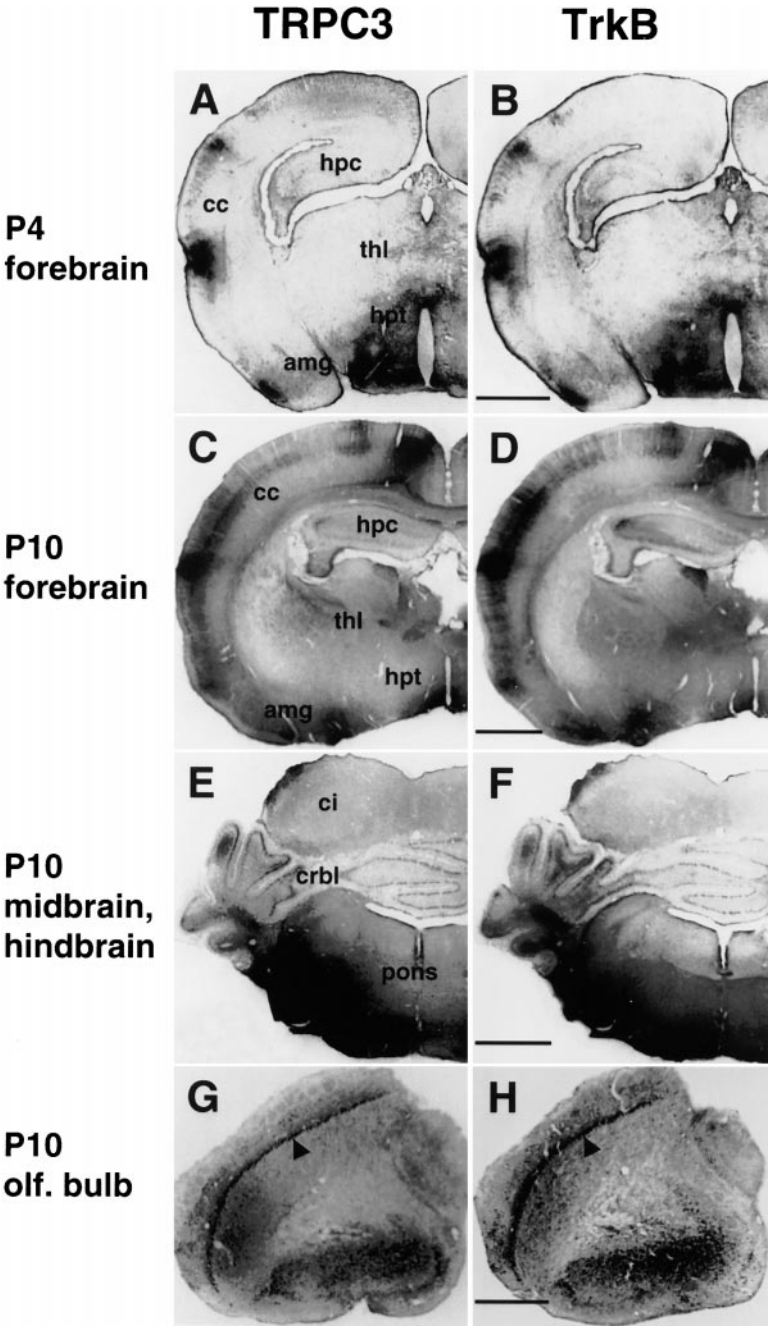

Figure 2. Comparison of the Spatial Distribution of TRPC3 and TrkB in Neonatal Rat Brains

Parallel sections from neonatal rat brains were stained with either anti-TRPC3 (A, C, E, and G) or anti-TrkB (B, D, F, and H) antibodies.
(A and B) P4 forebrains.
(C and D) P10 forebrains.
(E and F) P10 midbrain and hindbrain.
(G and H) P10 olfactory bulb ("olf. bulb").
Abbreviations: amg, amygdala; cc, cerebral cortex; ci, colliculus inferior; crbl, cerebellum; hpc, hippocampus; hpt, hypothalamus; and thl, thalamus. Scale bar, 1 mM (A–F) and 0.5 mM (G and H).

low concentration in the pipette solution, the outward current at positive potentials appeared to be carried only by Cs^{2+}. Based on this assumption, the relative permeability of Na^+ and Cs^+ (P_{Na^+}:P_{Cs^+}) was 1.1:1.0.

To characterize I_{BDNF} further, we performed single-channel recordings on the pontine neurons using the cell-attached mode. Before application of BDNF, no single-channel current was detected (Figure 5A). However, 1.2 ± 0.7 min (n = 9) following a 30 s stimulation with BDNF, an inward single-channel current appeared (Figures 5B and 5K). The amplitude of this current was 1.9 ± 0.3 pA (n = 9) with the voltage clamped at 5 mV. After withdrawing the pipette to create an inside-out patch, the current returned when the intracellular face of the patch was immersed in the normal Ca^{2+}-containing solution and the membrane potential was clamped at −70 mV (Figures 5C, 5K, and 5L; 1.9 ± 0.2 pA, n = 9 of 9). The mean open-time of the single channels was 19 ms (Figure 5E; n = 9). The single-channel conductance, determined with a voltage ramp between −70 to +70 mV, was 27.1 ± 0.2 pS (Figure 5F; n = 9), with a reversal potential at 0 mV (Figure 5J). After replacing all of the cations in the bath solution with N-methyl-D-glucamine (NMDG), the outward current was eliminated (Figures 5G and 5J; n = 6 of 6). Therefore, the single-channel currents appeared to be carried by cations rather than

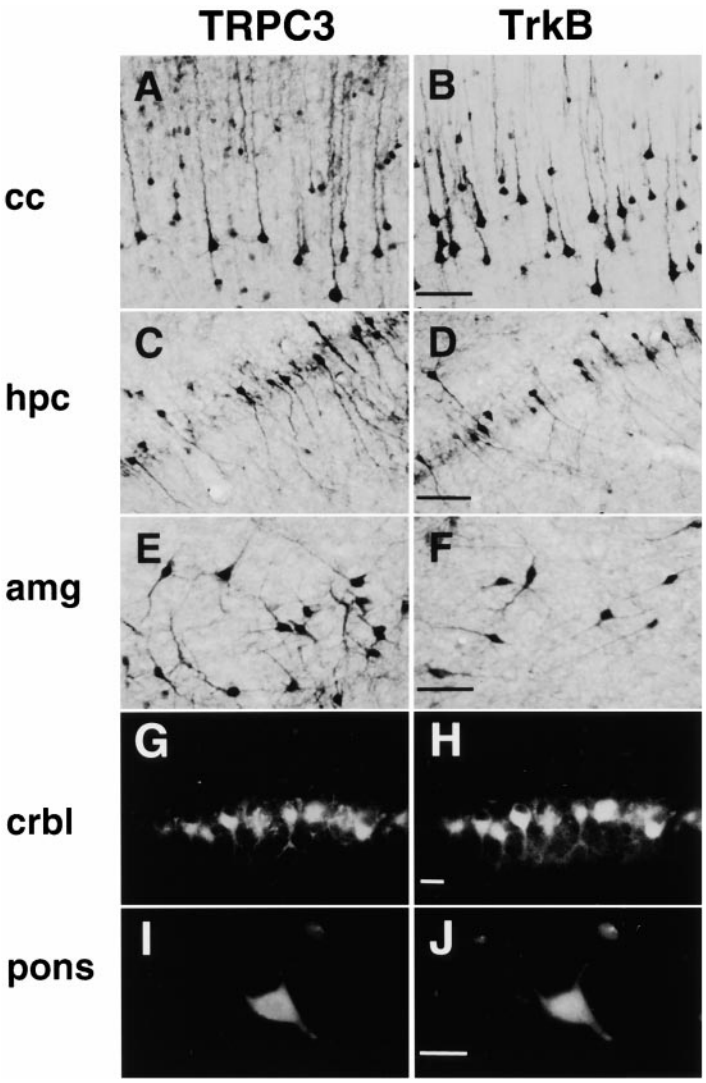

Figure 3. Comparison of the TRPC3 and TrkB Neuronal Expression Patterns

Tissue sections (from P10 rats) and isolated neurons (from P5 rats) were stained with anti-TRPC3 (A, C, E, G, and I) and/or anti-TrkB (B, D, F, H, and J) antibodies. Sections in (A) through (F) were stained in parallel. Other sections (G and H) and isolated pontine neurons ([I and J]; n = 1,422) were double labeled. See the legend to Figure 2 for abbreviations. Scale bar, 40 μm (A–F) and 10 μm (G–J).

Cl^-. Because the amplitudes of the single-channel currents in the normal solution (containing Ca^{2+}, Mg^{2+}, and Na^+; Figure 5F; 1.9 ± 0.2 pA, n = 9 of 9) and the Na^+ solution (containing Na^+ only; Figure 5H; 1.8 ± 0.3 pA, n = 6 of 6) were similar at +70 mV, it appeared that Na^+ was the major permeant ion. While there were many channel openings in a normal bath solution (Figure 5C; NP_o = 0.27, n = 9), few opening events were detected after changing to a Ca^{2+}-free solution (Figure 5D; NP_o = 0.02, n = 7 of 7). These latter data suggested that the BDNF-induced current was Ca^{2+} dependent.

The features of the BDNF-induced single-channel conductance resembled the whole-cell conductance. As was observed during the whole-cell recordings, the single-channel current amplitude obtained in a bath solution containing Cs^+ as the only cation was similar to that observed in the Na^+ solution (Figures 5H, 5I, and 6K; P_{Na^+}:P_{Cs^+} was 1.0:1.0). Furthermore, the delay in the BDNF-induced response (Figure 5K; 1.2 ± 0.7 min) was similar to that obtained during the whole-cell recording (Figure 4A; 1.2 ± 0.6 min; n = 16).

I_{BDNF} Was Mediated by TRPC3 Channels

Several properties of I_{BDNF} resembled the TRPC3 current that has been characterized in vitro (Zhu et al., 1996; Zitt et al., 1997; Hurst et al., 1998; Kiselyov et al., 1998; Zhu et al., 1998). These included a lack of Ca^{2+} selectivity, a reversal potential near 0 mV, and Ca^{2+} dependence. Inhibition of I_{BDNF} by SKF 96365 (Figure 6A; reduced to 19% ± 9% of the current without the drug, n = 6 of 8), a known inhibitor of store-operated Ca^{2+} entry and of TRPC3 in vitro (Merritt et al., 1990; Zhu et al., 1998) provided additional evidence the TRPC3 contributed to the BDNF-induced current.

A further indication that TRPC3 participated in I_{BDNF} was that TRPC3 and Trk receptors coimmunoprecipitated (co-IPed) from neonatal rat brain tissue (Figure 6B). The IPs were performed with pan-Trk antibodies, which recognize TrkA, TrkB, and TrkC since the available TRPC3 or TrkB antibodies were not effective in IPs (data not shown). TRPC3 did not co-IP after performing IPs with antibodies to the AMPA receptor subunit GluR2/3 (Figure 6B) or to bFGFR (data not shown). These data

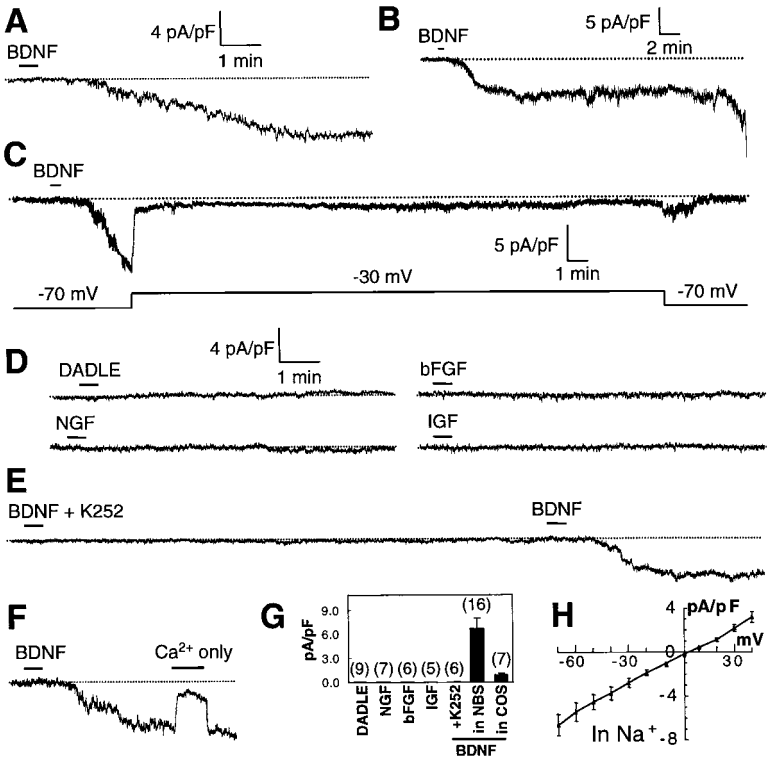

Figure 4. BDNF Induced a Cation Current (I_{BDNF}) in Isolated Pontine Neurons from P3–P8 Rats

Cells were clamped at −70 mV, and leak currents were subtracted. The pipettes contained the NPS in (A) through (G) and the Cs^+ solution (CPS) in (H). The periods during which the drugs were applied are indicated.

(A) BDNF (100 ng/ml) induced an inward current (n = 16 of 18).

(B) When the cells were clamped at −70 mV, they did not recover from the BDNF-induced response and died after 25 ± 7 min (indicated by the abrupt downward deflection; n = 8 of 8).

(C) To protect the cells from death after I_{BDNF} appeared, the voltage clamp was switched from −70 to −30 mV for 27 min, and then the holding potential was returned to −70 mV. With this paradigm, four of five cells were protected from cell death.

(D) Current was not induced by DADLE (2 μM; n = 9 of 9), NGF (100 ng/ml; n = 7 of 7), bFGF (100 ng/ml; n = 6 of 6), or IGF (100 ng/ml; n = 5 of 5).

(E) No current was produced upon coapplication of BDNF (100 ng/ml) and K252a (200 nM). Subsequent application of BDNF alone (100 ng/ml) induced I_{BDNF}.

(F) I_{BDNF} was only partially carried by Ca^{2+}. Switching from the NBS (2.5 mM Ca^{2+}) to the COS abolished most but not all of the current (n = 7 of 8).

(G) Average currents of whole-cell recordings shown in (A) and in (D) through (F). Each bar shows the average current (pA/pF) based on the indicated number of cells (n). The error bars indicate the standard errors of the mean. The proportion of cells that displayed characteristics represented by the sample traces in (A) through (F) (and that were included in the current averages) is indicated above.

(H) I–V relationship of I_{BDNF}. A set of voltages from −70 to +40 mV was applied in the presence of a NOS (n = 7). The standard errors of the mean are shown.

suggested that TRPC3 associated, either directly or indirectly, with at least one type of Trk receptor and were consistent with the data suggesting that BDNF led to the activation of TRPC3.

To provide additional evidence that TRPC3 contributed to the BDNF-induced cation influx, we tested whether the TRPC3 antibodies could modulate the conductances described above. These analyses were performed by adding either the $\alpha TRPC3^{N213}$ or control antibodies to the recording pipette and assessing the effects on the whole-cell currents. If the $\alpha TRPC3^{N213}$ antibodies had any effect, our expectation was that it would be inhibitory. However, we found that rather than having an inhibitory effect, the TRPC3 antibodies enhanced the whole-cell current. In several neurons exposed to $\alpha TRPC3^{N213}$ in the recording pipette, a slow inward current appeared even before the BDNF application (3 of 18 cells; data not shown). However, introduction of the antibodies prior to the application of BDNF typically had no affect (15 of 18 cells; data not shown). Upon addition of BDNF to cells containing $\alpha TRPC3^{N213}$, there was a 120% ± 48% enhancement in the current (an increase of 2.2-fold; Figures 6D and 6F; 15.0 ± 3.3 pA/pF, n = 14 of 15) relative to cells that were recorded in the absence of antibodies (Figures 6C and 6F; 6.8 ± 1.4 pA/pF, n = 16 of 18). The voltage-dependent K^+ and Na^+ currents were not affected by addition of $\alpha TRPC3^{N213}$ (see insets in Figures 6C, 6D, and 6F). Furthermore, no increase in current occurred due to addition of control IgY and antibodies that react with an intracellular portion of GluR2/3 (Figures 6E and 6F; 7.0 ± 1.6 pA/pF, n = 10 of 12).

The effect of $\alpha TRPC3^{N213}$ on cation influx was examined in greater detail by examining the single-channel currents in inside-out patches after adding the $\alpha TRPC3^{N213}$ antibodies to the bath solution. As described above, the single-channel activity was immediately and drastically diminished as a consequence of removing the Ca^{2+}-containing solution and switching to a Ca^{2+}-free solution (Figure 5D). However, of primary significance here, addition of the $\alpha TRPC3^{N213}$ antibodies to the Ca^{2+}-free solution quickly recovered the current (Figures 6G and 6I). Moreover, the channel activity was higher than that observed in the presence of Ca^{2+} (Figure 6I; NP_o = 0.59 ± 0.04, n = 6 of 6; as compared with 0.27 ± 0.03, n = 9 of 9). In contrast to the effect of $\alpha TRPC3^{N213}$, the control IgY and glutamate receptor antibodies, which were free of $\alpha TRPC3^{N213}$, had no significant effect on the single-channel current (Figures 6H and 6I; NP_o = 0.03 ± 0.03, n = 7 of 7). The $\alpha TRPC3^{N213}$ antibodies appeared to activate the same channels as BDNF since the conductances in Na^+ solution (Figure 6K; 26.9 ± 0.2 pS, n = 5; and 26.9 ± 0.2 pS, n = 4, respectively) and relative permeabilities to Na^+ and Cs^+ were the same under both sets of conditions (1.0:1.0 for both; Figure 6K; n = 5 and 4, respectively). In addition, the BDNF- and $\alpha TRPC3^{N213}$-induced currents displayed the same mean current amplitudes (Figure 6J; 1.9 ± 0.2 pA and

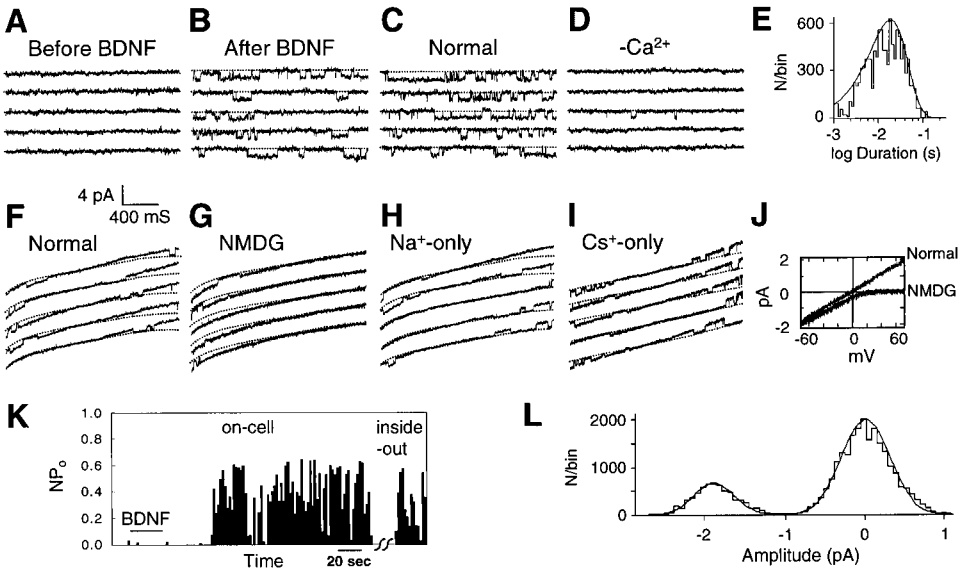

Figure 5. Single-Channel Analyses of BDNF-Induced Current in Pontine Neurons

The dotted lines indicate the closed state. The pipette contained NBS.

(A) No current was detected before application of BDNF (cell-attached mode with the voltage clamped at 5 mV).

(B) BDNF (100 ng/ml for 30 s) stimulated an inward current of 1.9 pA (n = 9).

(C–J) After the BDNF-stimulated current appeared, inside-out patches were generated, and channel activity was recorded with the membrane potential clamped at −70 mV.

(C) Channel activity in NBS (n = 9).

(D) Immediately after switching to the Ca^{2+}-free solution (n = 7), the channel activity decreased dramatically.

(E) Duration histogram of the single-channel open-state in NBS. The mean open-time obtained by a monoexponential fit was 19 ms.

(F–I) Channels were permeable to Na^+ and Cs^+. The ramp currents were recorded over a range of −70 to +70 mV.

(F) Ramp current in NBS (n = 9).

(G) Ramp current in an NMDG bath solution after treatment with anti-TRPC3 antibodies (n = 6; see text for explanation).

(H) Same as (G), except that the bath contained NOS (n = 6).

(I) Same as (G), except that the NMDG in the bath solution was replaced with 140 mM Cs^+ (n = 4).

(J) The I–V curves were generated in the NBS and NMDG solutions with the PulseFit program (HEKA Elektronik).

(K) The time course of single-channel activity (shown as open-probability) stimulated by 100 ng/ml BDNF at 5 mV. The later inside-out recording was performed at −70 mV in the same NBS.

(L) The amplitude distribution of the inside-out current was determined using cells voltage-clamped at −70 mV in NBS. A mean amplitude of 1.9 pA was calculated, using a monoexponential fit.

1.9 ± 0.3 pA, respectively) and reversal potentials at 0 mV in the normal bath solution (Figure 5J; data not shown).

To provide further evidence for the involvement of TRPC3 in I_{BDNF}, we tested whether BDNF could activate a TRPC3-dependent conductance in a heterologous expression system. The effects of adding BDNF were determined by performing whole-cell recordings after expressing TRPC3 and TrkB either individually or in combination in 293T cells. Consistent with the proposal that TRPC3 participated in I_{BDNF}, we found that addition of BDNF to cells coexpressing TrkB and TRPC3 displayed an increase in cation influx (Figure 7A; 7.9 ± 1.6 pA/pF, n = 11 of 14). The BDNF-induced influx required both TrkB and TRPC3 since addition of BDNF had no effect on cells expressing just TRPC3 (Figures 7B and 7D; 0.1 ± 0.1 pA/pF, n = 11 of 11) or TrkB (Figures 7C and 7D; 0.2 ± 0.2 pA/pF, n = 15 of 15). Although application of BDNF to cells expressing TRPC3 alone did not increase cation influx, introduction of TRPC3 in 293T cells resulted in an increase in basal cation influx (data not shown) as has been previously shown to be the case in 293 cells (Hurst et al., 1998; Zhu et al., 1998). The BDNF-induced current in 293T cells, which was characterized by a reversal potential at 0 mV and similarities in the permeabilities of Na^+ and Cs^+ (Figure 7E), resembled the previously described currents resulting from in vitro expression of TRPC3 (Zitt et al., 1997; Hurst et al., 1998).

I_{BDNF} Was Blocked by Inhibitors of PLC and IP_3 Receptors

Blockade of the BDNF-dependent current (Figures 8A and 8F; 0.2 ± 0.1 pA/pF, n = 7 of 7 cells) by introduction of the PLC inhibitor U73122 (Chen et al., 1994) provided evidence that I_{BDNF} was mediated through PLCγ. This effect was reversible since the current was restored after subsequent application of BDNF alone (Figure 8A). The mechanism through which stimulation of PLC is coupled to activation of TRPC3 is controversial. According to one recent study, TRPC3 channels expressed in HEK293 cells interact with the IP_3 receptor and are activated through release of Ca^{2+} from internal stores (Kiselyov et al., 1998). Contrary to these results, TRPC3 expressed in a different cell line, CHO-KI cells, appears to be activated by DAG rather than through depletion of Ca^{2+} from the intracellular stores (Hofmann et al., 1999).

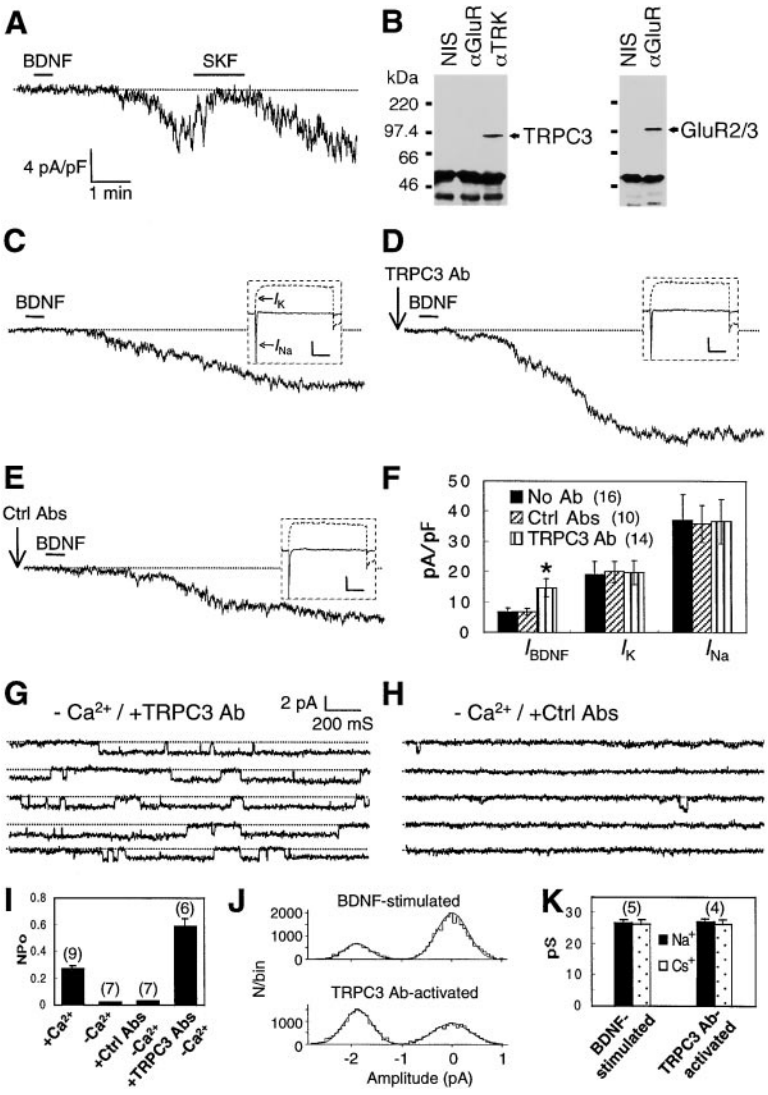

Figure 6. I_{BDNF} Was Mediated by TRPC3

The recordings were performed using pontine neurons isolated from neonatal rats.

(A) I_{BDNF} was inhibited by 30 μM SKF 96365 (n = 6 of 8 cells).

(B) TRPC3 co-IPed with Trk from P5 rat brains. IPs were performed with either nonimmune serum (NIS), anti-GluR2/3 antibodies (αGluR), or pan-Trk (αTrk) antibodies. The left panel is a Western blot of the IPs probed with anti-TRPC3 antibodies. The right panel showed that GluR2/3 IPed with the anti-GluR2/3 antibodies (the Western blot was probed with anti-GluR2/3 antibodies).

(C) Whole-cell current induced by BDNF (100 ng/ml; n = 16 of 18). The insert shows the voltage-dependent Na^+ and K^+ currents, which were recorded before the addition of BDNF. The Na^+ current was recorded after stepping the membrane potential from −70 to −40 mV, and the K^+ current was subsequently recorded after an additional step to +40 mV.

(D) Addition of $\alpha TRPC3^{N213}$ antibodies to the pipette (0.5 μg/ml) resulted in a 2.2-fold increase in current (120% ± 48% enhancement, n = 14 of 15).

(E) Control antibodies (Ctrl Abs) added to the pipette did not affect I_{BDNF}. The control antibodies consisted of a combination of chicken IgY (0.5 μg/ml) and anti-GluR2/3 antibodies (diluted in the pipette 1:1000; n = 10 of 12).

(F) Histograms showing the different effects of $\alpha TRPC3^{N213}$ on several types of currents. The error bars indicate the standard errors of the mean.

(G) Addition of $\alpha TRPC3^{N213}$ recovered the current in inside-out patches in a Ca^{2+}-free bath solution (n = 6). The conditions were identical to those in Figure 5D, except that $\alpha TRPC3^{N213}$ (0.1 μg/ml) was added to the bath solution.

(H) Addition of control antibodies did not recover the current. Conditions were identical to those in (G), except that control antibodies (IgY [0.1 μg/ml] and anti-GluR2/3 antibodies diluted 1:5000) were substituted for $\alpha TRPC3^{N213}$ (n = 7).

(I) The averaged open-probabilities of the inside-out patches treated with different bath solutions after BDNF stimulation. The standard errors of the mean are shown.

(J) Amplitude histograms indicating that the TRPC3 antibodies (lower; 1.9 ± 0.3 pA) activated the single channels with the same amplitude as BDNF (upper; 1.9 ± 0.2 pA). The data in the upper and lower panels were obtained with or without Ca^{2+} in the bath, respectively.

(K) Comparison between the conductances of the BDNF-stimulated single-channel openings and those activated by $\alpha TRPC3^{N213}$ in the Ca^{2+}-free bath solution. The conductances were measured between 0 and 70 mV with the patches in either NOS or COS.

Scale bar, 10 pA/pF and 50 ms ([C–E], inset).

I_{BDNF} did not appear to be mediated by DAG since the membrane-permeable DAG analog OAG (1-oleoyl-2-acetyl-sn-glycerol), which stimulated the TRPC3-dependent cation influx in CHO-KI cells (Hofmann et al., 1999), did not induce cation influx in primary pontine neurons (Figures 8B and 8G; 0.1 ± 0.1 pA/pF, n = 7 of 7 cells). However, inclusion of IP_3 in the recording pipette induced a current (n = 8 of 10 cells) with a latency (1.0 ± 0.5 min; Figure 8C) and amplitude (4.9 ± 1.0 versus 6.8 ± 1.4 pA/pF; Figure 8G) similar to that of I_{BDNF} but of shorter duration (7.8 ± 1.4 min; Figure 7C). Therefore, I_{BDNF} did not appear to be mediated simply by IP_3. No augmentation of the current was observed upon combined introduction of IP_3 and OAG (data not shown). Nevertheless, I_{BDNF} was inhibited by the membrane-permeable inhibitor of IP_3 receptors, xestospongin C (Gafni et al., 1997) ("Xest C"; Figures 8D and 8F; 0.2 ± 0.1 pA/pF, n = 6 of 6) as well as by another IP_3 receptor antagonist, heparin (Figures 8E and 8F; 0 pA/pF, n = 7 of 7). Thus, I_{BDNF} may be activated through a store-operated mechanism.

Discussion

TRPC3 Appears to Be a Subunit of the Channel that Mediates I_{BDNF}

A multitude of PLC-dependent Ca^{2+}-selective and -nonselective cation influx currents have been described from a wide variety of vertebrate cell types (Parekh and Penner, 1997). Some of these conductances appear to be regulated by release of Ca^{2+} from the internal stores, while others are not. The channels responsible for these

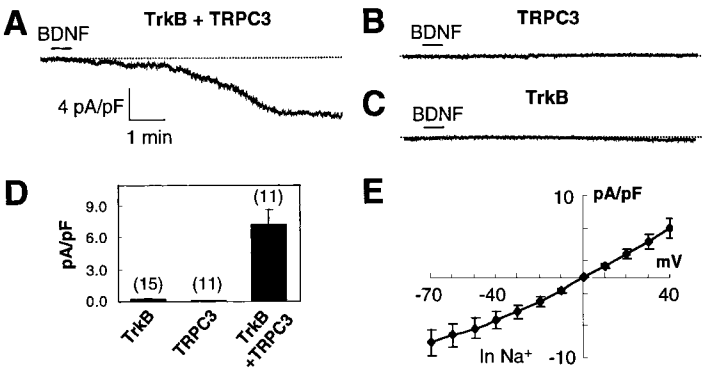

Figure 7. BDNF Induced a Cation Current in 293T Cells Expressing TrkB and TRPC3

The pipette solution was NPS (A–D) or CPS (E).

(A) BDNF-induced current in cells cotransfected with TrkB and TRPC3. Application of 100 ng/ml BDNF induced an inward cation current at −70 mV that had a delay of 1.3 ± 0.6 min (n = 11 of 14).

(B and C) BDNF did not elicit any significant effect in cells transfected with either TRPC3 (n = 11 of 11) or TrkB (n = 15 of 15) alone.

(D) Histogram showing the conductances after application of BDNF to cells transfected with TrkB and TRPC3, alone and in combination.

(E) I–V curve of the BDNF-induced currents in cells expressing both TrkB and TRPC3 (n = 7). The pipette and bath solutions are CPS and NOS, respectively. The leak currents were measured before BDNF application and were subtracted. The error bars (D and E) indicate the standard errors of the mean.

PLC-dependent currents have yet to be fully described; however, the vertebrate TRPC proteins are prime candidates. Expression of the TRPC channels in vitro leads to conductances that resemble many of the features of native Ca^{2+} and cation influx conductances. Nevertheless, it has not been demonstrated whether any of the TRPC channels contribute in neurons to PLC-dependent cation conductances.

In the current work, we provide evidence that TRPC3 is a subunit of a BDNF-activated channel in CNS neurons. In support of this conclusion, addition of BDNF led to the production of a PLC-dependent cation influx reminiscent of TRPC-mediated currents in vitro (see below). Moreover, I_{BDNF} was blocked by a known inhibitor of TRPC channels, SKF 96365 (Merritt et al., 1990; Kiselyov et al., 1998; Zhu et al., 1998). TrkB and TRPC3 not only colocalized in the same pontine neurons but also co-IPed from rat brains, indicating that the two proteins interact in a complex. The increase in the amplitude of the current in whole-cell recordings by addition of antibodies against TRPC3 provides further evidence that TRPC3 is a subunit of the channel responsible for BDNF. Moreover, the anti-TRPC3 antibodies were able to induce the single-channel conductance under conditions in which virtually no current was observed in the absence of antibodies or in the presence of control antibodies. Activation of an ion channel by antibodies is not unprecedented since the glutamate receptor channel

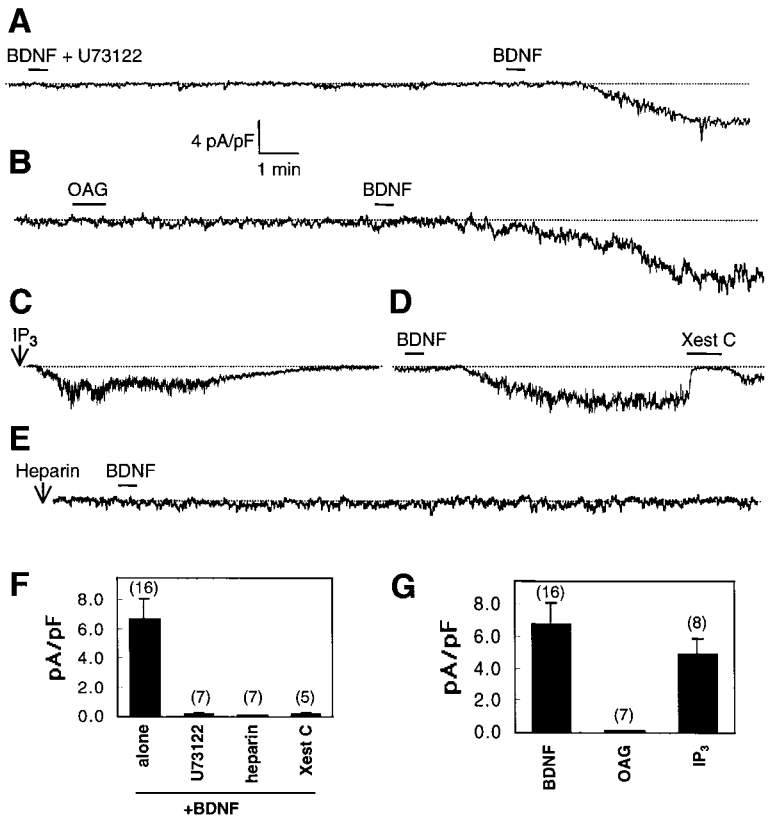

Figure 8. I_{BDNF} Was Blocked by Inhibitors of PLC and IP_3 Receptors

Whole-cell currents were recorded at −70 mV, using pontine neurons from neonatal rats.

(A) U73122 (2 μM; n = 7 of 7) blocked I_{BDNF}. Current was induced upon subsequent application of BDNF alone.

(B) OAG (50 μM; n = 7 of 7) failed to induce an inward current. Subsequent application of BDNF produced I_{BDNF}.

(C) Current produced upon inclusion of IP_3 (1 μM; n = 8 of 10) in the pipette.

(D) Xestospongin C (Xest C; 20 μM) inhibited I_{BDNF} (n = 6 of 6).

(E) Addition of heparin (100 μg/ml added to the pipette; n = 7 of 7) prevented the production of I_{BDNF}. In the absence of heparin, 2 of 18 cells did not respond to BDNF.

(F) Summary of the inhibitory effects of the drugs on I_{BDNF}. The total cell numbers tested are shown above each bar.

(G) Comparison of the current amplitudes produced by BDNF, OAG, and IP_3. The error bars (F and G) indicate the standard errors of the mean.

GluR3 can also be provoked by specific antibodies (Twyman et al., 1995). Further support for the proposal that TRPC3 was a channel subunit that contributed to I_{BDNF} was provided by in vitro expression studies. We found that BDNF stimulated a cation influx in 293T cells expressing both TrkB and TRPC3. However, addition of BDNF had no effect when applied to cells expressing just TrkB or TRPC3. Nevertheless, it cannot be formally excluded that TRPC3 is a cofactor rather than a channel subunit required for I_{BDNF}. Although TRPC3 has an overall predicted structure of six transmembrane domains (Vannier et al., 1998), which is reminiscent of many members of the superfamily of voltage-gated and second messenger–gated ion channels (Jan and Jan, 1992), it has not been ascertained whether any TRPC protein is capable of directing ion conductances after insertion of the purified protein into lipid bilayers.

Activation of TrkC may also give rise to a nonselective cation conductance in pontine neurons since application of the ligand for TrkC, NT-3, elicited a current with characteristics similar to those of I_{BDNF} but smaller in magnitude. Alternatively, the smaller response with NT-3 may also have been due to activation of TrkB since NT-3 can also bind to TrkB (Fariñas et al., 1998). However, stimulation of TrkA did not appear to lead to a similar nonselective cation influx since there was no stimulation of cation influx upon addition of the TrkA ligand NGF to a cell line, PC-12 cells, that expresses TrkA (H.-S. L. et al., unpublished data).

The characteristics of the endogenous current in pontine neurons, I_{BDNF}, are similar but not identical to the currents generated after expression of TRPC3 in vitro. Both the in vitro (current report; Zhu et al., 1996, 1998; Zitt et al., 1997; Hurst et al., 1998) and native currents are nonselective cation conductances that depend on activation of PLC and display reversal potentials near 0 mV. Additionally, as was observed in recent in vitro studies of TRPC3 (Kiselyov et al., 1998; Zhu et al., 1998), I_{BDNF} was inhibited by SKF 96365. However, I_{BDNF} was characterized by a much longer mean open-time ($\sim$20 versus $<$2 ms) and a smaller conductance (27 and 60 pS, respectively) than the in vitro TRPC3-dependent current. The differences in properties between the endogenous and in vitro conductances could reflect heteromultimerization between TRPC3 and other TRPC channels in the pontine neurons. We have previously shown that *Drosophila* TRP and TRPL are capable of forming heteromultimers (Xu et al., 1997). Moreover, several features of the conductance generated by the TRP/TRPL heteromultimers are distinct from either the TRP or TRPL homomeric conductances (Xu et al., 1997). Although the spatial distributions of the other TRPC proteins have not been determined, with the possible exception of TRPC2, which is a pseudogene in humans (Wes et al., 1995) but not in rodents (Liman et al., 1999; Vannier et al., 1999) or bovine (Wissenbach et al., 1998), all of the *TRPC* RNAs are expressed in the brain (Wes et al., 1995; Zhu et al., 1995, 1996; Funayama et al., 1996; Garcia and Schilling, 1997; Mori et al., 1998; Philipp et al., 1998). Furthermore, in situ hybridizations indicate that the expression patterns of the *TRPC3* and *TRPC4* RNAs are very similar in many brain tissues, including the pons (Mori et al., 1998). While it remains to be determined whether TRPC3 heteromultimerizes with other TRPC proteins in vivo, TRPC3 is capable of interacting with another TRPC protein, TRPC1, in vitro (Xu et al., 1997).

I_{BDNF} Is Activated through a Pathway Involving PLC and the IP_3 Receptor

While there is a consensus that TRPC channels are activated in vitro through stimulation of PLC, the mechanism(s) that couples TRPC-dependent cation influxes to PLC activation has been controversial. Recently, TRPC3 has been expressed in vitro by two different groups, and the conclusions of these studies were quite disparate. TRPC3 is activated in CHO-K1 cells by a membrane-permeable analog of DAG (OAG) and not through production of IP_3 or via a store-operated mechanism (Hofmann et al., 1999). By contrast, TRPC3 appears to be activated through a store-operated mechanism in HEK293 cells (Kiselyov et al., 1998). In this latter study, TRPC3 was found to be activated by IP_3, and the current was blocked by two inhibitors of the IP_3 receptor: heparin and xestospongin C. Moreover, evidence was provided that TRPC3 and the IP_3 receptors interact (Kiselyov et al., 1998).

We investigated the mechanism by which the TRPC3-dependent current may be activated in vivo. We found that I_{BDNF} appeared to be coupled to activation of PLC since the current was reversibly blocked by the PLC inhibitor U73122. Furthermore, I_{BDNF} was not induced by OAG and was blocked by heparin and xestospongin C. Application of IP_3 induced a current similar to I_{BDNF} but shorter in duration. Thus, IP_3 appears to be required but was not sufficient for maximal activation of I_{BDNF}. The current was not further augmented by coapplication of OAG and IP_3. Thapsigargin had no effect (H.-S. L. et al., unpublished data); however, the thapsigargin-induced release is slower than with IP_3. Moreover, this drug inhibits the Ca^{2+}-ATPase in the smooth endoplasmic reticulum and causes Ca^{2+} release via the leak current rather than through the IP_3 receptor. Thus, the lack of induction of I_{BDNF} by thapsigargin could be due to a requirement for rapid release of Ca^{2+} from the internal stores and/or release via the IP_3 receptor.

The present study represents an in vivo analysis of a TRPC-dependent current, and the results indicate that TRPC3 is activated in pontine neurons through a pathway that involves TrkB, PLCγ, production of IP_3, the IP_3 receptor, and intracellular Ca^{2+}. These requirements for the BDNF-induced cation influx suggest that TRPC3 is activated in vivo according to a store-operated mechanism. Although TRPC3 appears to be activated through a TrkB-dependent pathway in pontine neurons, this may not be the only mode through which TRPC3 is stimulated in vivo. TRPC3 can be activated in vitro through receptors, such as the M5 muscarinic receptor, that are coupled to PLC-β (Zhu et al., 1996). Thus, activation of TRPC3 in vivo may occur through several types of receptors that lead to stimulation of PLC.

Potential Function of I_{BDNF}

Several previous studies have indicated that application of BDNF leads to increases in intracellular Ca^{2+}. In some cases, the elevation appears to arise from release of Ca^{2+} from the internal stores (Tao et al., 1998). There is also evidence that neurotrophins can stimulate Ca^{2+} influx through voltage-gated Ca^{2+} channels and NMDA receptors (reviewed by Berninger and Poo, 1996). However, another major mode of Ca^{2+} entry into neurons may be through the TRPC channels. As mentioned above, a

minimum of five *TRPC* RNAs are expressed in the brain, and three appear to be highly enriched in the CNS. These observations, combined with the findings that TRPC3 contributes to a PLC-dependent cation influx in CNS neurons, raise the possibility that other TRPC conductances may also contribute significantly to Ca^{2+} entry in CNS neurons.

A question raised by the current work concerns the role of the BDNF-induced cation conductance in the CNS. Activation of neurotrophin receptors induces a variety of effects in the nervous system. These include a multitude of long-term changes in the developing nervous system, such as differentiation, cell proliferation, and survival, which typically occur after a significant delay of up to many hours following stimulation of the neurotrophin receptors (reviewed by Reichardt and Fariñas, 1997). Many of these effects are mediated through transcriptional induction of distinct sets of genes (reviewed by Segal and Greenberg, 1996). Neurotrophins can also induce rapid effects, such as morphological changes at the growth cone and modulation of neurotransmitter release (reviewed by Berninger and Poo, 1996; Bonhoeffer, 1996; Shieh and Ghosh, 1997). These later changes, some of which are activity dependent, are rapid and occur on the order of one or a few minutes. The mechanisms underlying these fast responses to neurotrophins are not understood, but they are unlikely to occur through regulation of transcription. It is intriguing that the TRPC3 protein is expressed during a relatively narrow developmental window, before and after birth, during which a number of activity-dependent developmental changes occur.

We propose that some of the rapid responses that occur through activation of TrkB may be mediated by the TRPC3-dependent Ca^{2+} and Na^{+} influx. Cation influx through TRPC3 may modulate rapid processes, such as synaptic transmission, by altering the membrane potential, which in turn might facilitate Ca^{2+} entry through voltage-dependent channels and the NMDA receptor.

Experimental Procedures

Generation and Purification of TRPC3 Antibodies

To generate antibodies to TRPC3, we expressed a fusion protein consisting of the N-terminal 213 amino acids of TRPC3 fused to glutathione S-transferase. The fusion protein was fractionated by SDS–PAGE, electroeluted as described (Montell and Rubin, 1988), and introducted into chickens (Aves Lab). To purify the TRPC3 antibodies, we generated a fusion protein consisting of the maltose binding protein (MBP) linked to the same 213 N-terminal residues of TRPC3. The MBP–TRPC3 fusion was immobilized on amylose resin columns and eluted as described by the manufacturer (New England Biolabs). The MBP–TRPC3 was then coupled to CNBr-activated Sepharose 4B as described (Pharmacia), and the anti-TRPC3 antibodies were purified from the total IgY according to the instructions in the SulfoLink kit (Pierce). The IgY antibodies from which the TRPC3 antibodies were removed were saved to provide a control. Both antibody fractions were quantitated and used at the same concentration.

Cell Culture and Transfection

Transfections in 293T cells were performed with Lipofectamine (BRL). To perform Western blots, cells were lysed 36–48 hr posttransfection in IPB buffer (1% Triton X-100, 3× Complete [protease-inhibitor cocktail; Boehringer Mannheim], 137 mM NaCl, 2.7 mM KCl, 4.3 mM Na_2HPO_4, and 1.4 mM KH_2PO_4 [pH 7.3]) and centrifuged to remove cellular debris. For electrophysiological analysis, pTRPC3 and/or pTrkB were cotransfected into 293T cells together with a construct containing the *green fluorescent protein* (*GFP*) marker gene. The cells were plated onto coverslips 1 day later. The recordings were performed 36–68 hr posttransfection.

Western Blot Analyses of TRPC3 Expression in Various Tissues

Fetal and adult human cerebral cortices were obtained from the Brain and Tissue Bank for Developmental Disorders, University of Maryland School of Medicine and from the Johns Hopkins Hospital, respectively (Figure 1C). CD rats and CD-1 mice were products of the Charles River Lab. Various rat tissues were dissected from P5 rats (Figure 1D). The DRG and specific regions of the brain were obtained from P10 rats (Figure 1E). Tissues were homogenized in IPB buffer, and the extracts were centrifuged at 3,000 rpm to remove tissue debris and then centrifuged at 14,000 rpm for 20 min. The supernatants were saved for IPs (see below), and the pellets were dissolved in SDS sample buffer. The proteins in the samples were fractionated by SDS–PAGE and transferred to polyvinylidene difluoride (PVDF) membranes, and the membranes were probed with the appropriate primary antibodies and horseradish peroxidase– (HRP-) labeled secondary antibodies. Labeling of proteins was detected with the Renaissance enhanced chemiluminescence kit (Dupont, NEN). The same tissue extracts were reprobed with antibodies that recognize α- and β-tubulin (Clontech). The anti-TRPC3 antibodies (final concentration of 0.25 μg/ml) recognized TRPC3 in rats, mice, and humans.

Immunohistochemistry

The brains from neonatal rats were embedded in OCT compound (Tissue-Tek, Miles), and 25 μm frozen sections were transferred to microtiter dishes containing phosphate-buffered saline (PBS). The sections were washed once with PBS and immersed in PBST buffer (PBS plus 0.1% Triton X-100) for 10 min. After blocking with 1:10 BlokHen (for anti-TRPC3 antibodies; Aves Labs) or goat serum (for anti-TrkB antibodies) in PBST, the sections were incubated overnight in 2 μg/ml anti-TRPC3 or 2 μg/ml anti-TrkB antibodies (Santa Cruz). As a negative control, we used 2 μg/ml chicken IgY, from which the anti-TRPC3 antibodies were removed (see above). The sections were washed in PBST and incubated for 1 hr with biotin-labeled secondary antibodies diluted in PBST. To detect the signal, a universal HRP ABC kit (Vector Lab) was used. The DAB substrate reaction was performed in Tris-buffered saline in the presence of 0.03% $NiCl_2$. The sections were mounted on slides and dehydrated once in an ethanol series and twice in xylene.

To perform the double-labeling experiments, the cerebellar sections and isolated pontine neurons were incubated overnight (4°C) with the chicken anti-TRPC3 and rabbit anti-TrkB antibodies with the buffers and antibody concentrations described above. The samples were subsequently incubated for 1 hr with biotin-conjugated anti-chicken antibodies (1:300) plus FITC-labeled anti-rabbit antibodies (1:30) and then incubated with rhodamine-avidin (1:50) for an additional 1 hr.

Pontine Neuron Isolation

The pons were removed by microdissection from P3–P8 CD rats and minced in dissection solution (DS; in mM: NaCl, 135; KCl, 2.5; $MgCl_2$, 1.8; $CaCl_2$, 1; glucose, 25; cysteine, 1; and HEPES, 20 [pH 7.4]). The tissue debris were digested with 1 mg/ml trypsin in DS for 30 min at 37°C followed by 30 min at 30°C, with gentle shaking. The digested debris were transferred into DS containing 2 mg/ml trypsin inhibitor and triturated to disperse the neurons. The neurons were then transferred into the normal bath solution (NBS; in mM: NaCl, 140; $MgCl_2$, 1.2; $CaCl_2$, 2.5; glucose, 10; and HEPES, 14 [pH 7.4]) and plated onto 35 mm dishes for electrophysiology experiments or introduced onto 18 mm round coverslips for immunocytochemistry. The dishes and coverslips were precoated with polylysine.

Electrophysiology

Isolated neurons of similar size (20–24 pF) and containing at least three neurites, or isolated 293T cells expressing the GFP marker, were chosen for the recordings. The electrophysiology was performed with an Axopatch 200B amplifier (Axon Instruments) at 5 kHz filtration. The continual whole-cell currents were recorded with the MacLab 3.13 system (ADInstruments) at a sampling speed of

20 Hz. The step and single-channel currents were recorded under the control of a Pulse 8.09 program (HEKA Elektronik), and the single-channel currents were further filtered at 1 kHz with the same program. The capacitance and series resistance (<12 MΩ) were compensated.

The resistance of the pipette used in the whole-cell configuration was 2.5–3.0 MΩ. The normal pipette solution (NPS) contained (in mM): KCl, 140; $MgCl_2$, 2; EGTA, 10; ATP, 0.3; GTP, 0.03; and HEPES, 10 (pH 7.2). The membrane potential was clamped at −70 mV. For the I–V relationship studies, the KCl in the NPS was replaced with CsCl, and 2 μM tetrodotoxin was added (CPS). A set of step voltage commands (−70 to +40 mV, in 10 mV increments) was applied to the cells. The currents before BDNF application were subtracted from the later BDNF responses.

To perform the single-channel recordings, the pipette was filled with the NBS. The single-channel currents were activated by BDNF in the cell-attached configuration (5 mV). Once the BDNF current was detected, the pipette was withdrawn to create inside-out patches, and the current was recorded with the membrane potential clamped at −70 mV. A voltage ramp from −70 to +70 mV was generated to determine the I–V relationship.

Unless specified otherwise, recordings were performed with cells or membrane patches maintained in NBS. A 6-barrel drug application system was used to change the solution bathing the cells or membrane patches. The Ca^{2+}-only solution (COS) contained (in mM): $CaCl_2$, 2.5; glucose, 10; and HEPES, 14 (pH 7.4). The Ca^{2+}-free solution (CFS) was the same as the NBS, except that 2.5 mM EGTA was substituted for the $CaCl_2$. The Na^+-only solution (NOS) consisted of (in mM): NaCl, 140; EGTA, 2.5; glucose, 10; and HEPES, 14 (pH 7.4). The NMDG solution contained (in mM): NMDG, 140; EGTA, 2.5; glucose, 10; and HEPES, 14 (pH 7.4). The antibodies were dissolved in CFS. All other drugs were introduced in NBS.

The relative permeability of the whole-cell current was calculated according to the equation $P_{Na}:P_{Cs} = [Cs^+]_o \cdot e^{FV_{rev}/RT}/[Na^+]_o$. V_{rev} is the reversal potential when the pipette contained CPS and the bath solution was NOS. The relative permeability of the single-channel current was estimated as $P_{Na}:P_{Cs} = G_{Na}/G_{Cs}$. G_{Na} and G_{Cs} are the conductances for Na^+ and Cs^+, respectively, obtained in the approximate range of 0–70 mV. The single-channel recording data were analyzed with the TAC and TACfit programs (Skalar Instruments).

Coimmunoprecipitations

Rabbit pan-Trk antibodies (0.2 μg; Santa Cruz) or 1 μl of rabbit anti-GluR2/3 antibodies (a gift from Dr. R. Huganir) was added to 300 μl of P5 rat brain supernatants (see above) and rotated for 1 hr at 4°C. Protein A beads (20 μl; Sigma) were added to the tissue supernatant, and the samples were rotated for 1 hr at 4°C and centrifuged at 5,000 rpm for 1 min to pellet the beads. The beads were resuspended in 100 μl of protein sample buffer and boiled for 10 min. The proteins in the supernatants were fractionated by SDS–PAGE, transferred to PVDF membranes, and probed with either anti-TRPC3 or anti-GluR2/3 antibodies.

Acknowledgments

We thank R. Vigorito and H. R. Zielke at the Brain and Tissue Bank for Developmental Disorders, University of Maryland School of Medicine for the fetal brains and K. Lai of the Johns Hopkins Hospital for the adult brains. We also thank D. Ginty, A. Ghosh, and D. Montell for comments on this manuscript. This work was supported by a grant from the National Eye Institute (EY10852) to C. M.

Received April 8, 1999; revised August 4, 1999.

References

Barbacid, M. (1995). Neurotrophic factors and their receptors. Curr. Opin. Cell Biol. *7*, 148–155.

Berninger, B., and Poo, M. (1996). Fast actions of neurotrophic factors. Curr. Opin. Neurobiol. *6*, 324–330.

Berridge, M.J. (1995). Capacitative calcium entry. Biochem. J. *312*, 1–11.

Berridge, M.J. (1998). Neuronal calcium signaling. Neuron *21*, 13–26.

Bonhoeffer, T. (1996). Neurotrophins and activity-dependent development of the neocortex. Curr. Opin. Neurobiol. *6*, 119–126.

Boulay, G., Zhu, X., Peyton, M., Jiang, M.S., Hurst, R., Stefani, E., and Birnbaumer, L. (1997). Cloning and expression of a novel mammalian homolog of *Drosophila* transient receptor potential (Trp) involved in calcium entry secondary to activation of receptors coupled by the G_q class of G protein. J. Biol. Chem. *272*, 29672–29680.

Chen, P., Xie, H., Sekar, M.C., Gupta, K., and Wells, A. (1994). Epidermal growth factor receptor–mediated cell motility: phospholipase C activity is required, but mitogen-activated protein kinase activity is not sufficient for induced cell movement. J. Cell Biol. *127*, 847–857.

Fariñas, I., Wilkinson, G.A., Backus, C., Reichardt, L.F., and Patapoutian, A. (1998). Characterization of neurotrophin and Trk receptor functions in developing sensory ganglia: direct NT-3 activation of TrkB neurons in vivo. Neuron *21*, 325–334.

Fryer, R.H., Kaplan, D.R., Feinstein, S.C., Radeke, M.J., Grayson, D.R., and Kromer, L.F. (1996). Developmental and mature expression of full-length and truncated TrkB receptors in the rat forebrain. J. Comp. Neurol. *374*, 21–40.

Funayama, M., Goto, K., and Kondo, H. (1996). Cloning and expression localization of cDNA for rat homolog of TRP protein, a possible store-operated calcium (Ca^{2+}) channel. Mol. Brain Res. *43*, 259–266.

Gafni, J., Munsch, J.A., Lam, T.H., Catlin, M.C., Costa, L.G., Molinski, T.F., and Pessah, I.N. (1997). Xestospongins: potent membrane permeable blockers of the inositol 1,4,5-trisphosphate receptor. Neuron *19*, 723–733.

Garcia, R.L., and Schilling, W.P. (1997). Differential expression of mammalian TRP homologues across tissues and cell lines. Biochem. Biophys. Res. Commun. *239*, 279–283.

Hardie, R.C., and Minke, B. (1992). The *trp* gene is essential for a light-activated Ca^{2+} channel in Drosophila photoreceptors. Neuron *8*, 643–651.

Henderson, C.E. (1996). Role of neurotrophic factors in neuronal development. Curr. Opin. Neurobiol. *6*, 64–70.

Hofmann, T., Obukhov, A.G., Schaefer, M., Harteneck, C., Gudermann, T., and Schultz, G. (1999). Direct activation of human TRPC6 and TRPC3 channels by diacylglycerol. Nature *397*, 259–263.

Hurst, R.S., Zhu, X., Boulay, G., Birnbaumer, L., and Stefani, E. (1998). Ionic currents underlying HTRP3 mediated agonist-dependent Ca^{2+} influx in stably transfected HEK293 cells. FEBS Lett. *422*, 333–338.

Jan, L.Y., and Jan, Y.N. (1992). Tracing the roots of ion channels. Cell *69*, 715–718.

Kiselyov, K., Xu, X., Mozhayeva, G., Kuo, T., Pessah, I., Mignery, G., Zhu, X., Birnbaumer, L., and Muallem, S. (1998). Functional interaction between $InsP_3$ receptors and store-operated Htrp3 channels. Nature *396*, 478–482.

Klein, R., Parada, L.F., Coulier, F., and Barbacid, M. (1989). trkB, a novel tyrosine protein kinase receptor expressed during mouse neural development. EMBO J. *8*, 3701–3709.

Liman, E.R., Corey, D.P., and Dulac, C. (1999). TRP2: a candidate transduction channel for mammalian pheromone sensory signaling. Proc. Natl. Acad. Sci. USA *96*, 5791–5796.

Lo, D.C. (1995). Neurotrophic factors and synaptic plasticity. Neuron *15*, 979–981.

Martin-Zanca, D., Barbacid, M., and Parada, L.F. (1990). Expression of the trk proto-oncogene is restricted to the sensory cranial and spinal ganglia of neural crest origin in mouse development. Genes Dev. *4*, 683–694.

Merritt, J.E., Armstrong, W.P., Benham, C.D., Hallam, T.J., Jacob, R., Jaxa-Chamiec, A., Leigh, B.K., McCarthy, S.A., Moores, K.E., and Rink, T.J. (1990). SK&F 96365, a novel inhibitor of receptor-mediated calcium entry. Biochem. J. *271*, 515–522.

Montell, C. (1999). Drosophila visual transduction. Annu. Rev. Cell Dev. Biol. *15*, 231–268.

Montell, C., and Rubin, G.M. (1988). The Drosophila *ninaC* locus encodes two photoreceptor cell specific proteins with domains homologous to protein kinases and the myosin heavy chain head. Cell *52*, 757–772.

Montell, C., and Rubin, G.M. (1989). Molecular characterization of

the Drosophila *trp* locus: a putative integral membrane protein required for phototransduction. Neuron *2*, 1313–1323.

Montell, C., Jones, K., Hafen, E., and Rubin, G. (1985). Rescue of the *Drosophila* phototransduction mutation *trp* by germline transformation. Science *230*, 1040–1043.

Mori, Y., Takada, N., Okada, T., Wakamori, M., Imoto, K., Wanifuchi, H., Oka, H., Oba, A., Ikenaka, K., and Kurosaki, T. (1998). Differential distribution of TRP Ca^{2+} channel isoforms in mouse brain. Neuroreport *9*, 507–515.

Okada, T., Shimizu, S., Wakamori, M., Maeda, A., Kurosaki, T., Takada, N., Imoto, K., and Mori, Y. (1998). Molecular cloning and functional characterization of a novel receptor-activated TRP Ca^{2+} channel from mouse brain. J. Biol. Chem. *273*, 10279–10287.

Parekh, A.B., and Penner, R. (1997). Store depletion and calcium influx. Physiol. Rev. *77*, 901–930.

Peterson, C.C.H., Berridge, M.J., Borgese, M.F., and Bennett, D.L. (1995). Putative capacitative calcium entry channels: expression of *Drosophila trp* and evidence for the existence of vertebrate homologues. Biochem. J. *311*, 41–44.

Philipp, S., Cacalié, A., Freichel, M., Wissenbach, U., Zimmer, S., Trost, C., Marquart, A., Murakami, M., and Flockerzi, V. (1996). A mammalian capacitative calcium entry channel homologous to Drosophila TRP and TRPL. EMBO J. *15*, 6166–6171.

Philipp, S., Hambrecht, J., Braslavski, L., Schroth, G., Freichel, M., Murakami, M., Cavalié, A., and Flockerzi, V. (1998). A novel capacitative calcium entry channel expressed in excitable cells. EMBO J. *17*, 4274–4282.

Putney, J.W., Jr. (1993). Excitement about calcium signalling in inexcitable cells. Science *262*, 676–678.

Putney, J.W., Jr., and Bird, G.S. (1994). Calcium mobilization by inositol phosphates and other intracellular messengers. Trends Endocrinol. Metab. *5*, 256–260.

Reichardt, L.F., and Fariñas, I. (1997). Neurotrophic factors and their receptors: roles in neuronal development and function. In Molecular Approaches to Neural Development, M.W. Cowan et al., eds. (New York: Oxford University Press), pp. 220–263.

Segal, R.A., and Greenberg, M.E. (1996). Intracellular signaling pathways activated by neurotrophic factors. Annu. Rev. Neurosci. *19*, 463–489.

Shieh, P.B., and Ghosh, A. (1997). Neurotrophins: new roles for a seasoned cast. Curr. Biol. *7*, R627–R630.

Tao, X., Finkbeiner, S., Arnold, D.B., Shaywitz, A.J., and Greenberg, M.E. (1998). Ca^{2+} influx regulates BDNF transcription by a CREB family transcription factor–dependent mechanism. Neuron *20*, 709–726.

Thoenen, H. (1995). Neurotrophins and neuronal plasticity. Science *270*, 593–598.

Twyman, R.E., Gahring, L.C., Spiess, J., and Rogers, S.W. (1995). Glutamate receptor antibodies activate a subset of receptors and reveal an agonist binding site. Neuron *14*, 755–762.

Vaca, L., Sinkins, W.G., Hu, Y., Kunze, D.L., and Schilling, W.P. (1994). Activation of recombinant *trp* by thapsigargin in Sf9 insect cells. Am. J. Physiol. *266*, C1501-C1505.

Vannier, B., Zhu, X., Brown, D., and Birnbaumer, L. (1998). The membrane topology of human transient receptor potential 3 as inferred from glycosylation-scanning mutagenesis and epitope immunocytochemistry. J. Biol. Chem. *273*, 8675–8679.

Vannier, B., Peyton, M., Boulay, G., Brown, D., Qin, N., Jiang, M., Zhu, X., and Birnbaumer, L. (1999). Mouse trp2, the homologue of the human trpc2 pseudogene, encodes mTrp2, a store depletion-activated capacitative Ca^{2+} entry channel. Proc. Natl. Acad. Sci. USA *96*, 2060–2064.

Wes, P.D., Chevesich, J., Jeromin, A., Rosenberg, C., Stetten, G., and Montell, C. (1995). TRPC1, a human homolog of a *Drosophila* store-operated channel. Proc. Natl. Acad. Sci. USA *92*, 9652–9656.

Wissenbach, U., Schroth, G., Philipp, S., and Flockerzi, V. (1998). Structure and mRNA expression of a bovine trp homologue related to mammalian trp2 transcripts. FEBS Lett. *429*, 61–66.

Xu, X.-Z.S., Li, H.-S., Guggino, W.B., and Montell, C. (1997). Coassembly of TRP and TRPL produces a distinct store-operated conductance. Cell *89*, 1155–1164.

Yan, Q., Radeke, M.J., Matheson, C.R., Talvenheimo, J., Welcher, A.A., and Feinstein, S.C. (1997). Immunocytochemical localization of TrkB in the central nervous system of the adult rat. J. Comp. Neurol. *378*, 135–157.

Zhu, X., Chu, P.B., Peyton, M., and Birnbaumer, L. (1995). Molecular cloning of a widely expressed human homologue for the *Drosophila trp* gene. FEBS Lett. *373*, 193–198.

Zhu, X., Jiang, M., Peyton, M., Boulay, G., Hurst, R., Stefani, E., and Birnbaumer, L. (1996). *trp*, a novel mammalian gene family essential for agonist-activated capacitative Ca^{2+} entry. Cell *85*, 661–671.

Zhu, X., Jiang, M., and Birnbaumer, L. (1998). Receptor-activated Ca^{2+} influx via human Trp3 stably expressed in human embryonic kidney (HEK)293 cells. Evidence for a non-capacitative Ca^{2+} entry. J. Biol. Chem. *273*, 133–142.

Zitt, C., Zobel, A., Obukhov, A.G., Harteneck, C., Kalkbrenner, F., Lückhoff, A., and Schultz, G. (1996). Cloning and functional expression of a human Ca^{2+}-permeable channel activated by calcium store depletion. Neuron *16*, 1189–1196.

Zitt, C., Obukhov, A.G., Strubing, C., Zobel, A., Kalkbrenner, F., Lückhoff, A., and Schultz, G. (1997). Expression of TRPC3 in Chinese hamster ovary cells results in calcium-activated cation currents not related to store depletion. J. Cell Biol. *138*, 1333–1341.